Formation dynamics of gold nanoparticles measured by single-shot near-field heterodyne transient grating method

ARTICLE *in* CHEMICAL PHYSICS LETTERS · MAY 2008

Impact Factor: 1.9 · DOI: 10.1016/j.cplett.2008.04.014

3 AUTHORS, INCLUDING:

Kenji Katayama
Chuo University
95 PUBLICATIONS **806** CITATIONS

Chemical Physics Letters 457 (2008) 271–275

Contents lists available at ScienceDirect

Chemical Physics Letters

journal homepage: www.elsevier.com/locate/cplett

Formation dynamics of gold nanoparticles measured by single-shot near-field heterodyne transient grating method

Yuta Nakazato, Mitsuhide Okuda, Kenji Katayama *

Department of Applied Chemistry, Faculty of Science and Technology, Chuo University, 1-13-27 Kasuga, Bunkyo, Tokyo 112-8551, Japan

ARTICLE INFO

Article history:
Received 25 December 2007
In final form 4 April 2008
Available online 10 April 2008

ABSTRACT

The dynamic processes of photoreduction of chloroauric acid and subsequent formation of gold nanoparticles were directly observed by means of the single-shot, near-field heterodyne transient grating method. For a polyvinylpyrrolidone (PVP) concentration of less than 0.5 mM, the observed transient responses consisted of four exponential functions that corresponded to thermal decay and the reaction and diffusion processes of three chemical species in the photoreduction processes. Another exponential component was found for PVP concentrations above 0.5 mM, and it was proposed that this component corresponds to the diffusion of gold nanoparticles from the decay time dependence on the pump intensity.

The successful synthesis of an adequately monodispersed solution of gold nanoparticles in a liquid phase depends on the distinct separation of nucleation from growth processes [1–3]. To control the synthesis of nanoparticles, it is necessary to understand their formation mechanism. In general, the formation steps are classified into: (1) the reduction processes of chlorauric acid, (2) formation of nuclei, and (3) particle growth [4]. However, steps (1) and (2) have not been sufficiently clarified because the reaction is too fast and also it is difficult to detect the involved ionic species in real time. In contrast, step (3) is well-examined because the growth process of nanoparticles with diameters larger than several nanometers can be monitored by analyzing the characteristic plasmon absorption band using a conventional spectrometer [5,6].

Photochemical dynamics can be measured by flash photolysis, but few reports exist on the initial processes of photo-reduction of chlorauric acid and subsequent formation of nanoparticles under specific experimental conditions [7,8]. In general, it is difficult to measure this kind of irreversible reaction dynamics using flash photolysis, because the absorption changes due to the photo-reduced intermediate species are small, but repeated irradiation of pump pulses is necessary to obtain meaningful data for signal averaging. As a result, composition of the sample is changed due to the generation of photoproducts during the measurement.

The transient grating (TG) technique is another useful tool to detect the photo-induced reaction dynamics [9,10]. Since TG monitors the change in the refractive index, optically silent dynamics such as molecular volume change can be also monitored [11]. Recently, this technique was applied to investigate the formation dynamics of Pt nanoparticles [12], and the temporal change of the transient responses, of the order of minutes, was used to follow the growth processes.

We recently developed the near-field heterodyne transient grating (NF–HD–TG) method [13–17], which features a simple optical setup and highly sensitive detection using a heterodyne technique. In this study, we developed a single-shot method for detecting the NF–HD–TG signal to directly observe irreversible reaction dynamics; in this case, the photoreduction of chlorauric acid and the subsequent formation of gold nanoparticles.

The principle of the NF–HD–TG method was described in detail in previous papers [17–19]. The main feature is that temporal responses of the real ($\Delta n(t)$) and imaginary parts ($\Delta k(t)$) of the refractive index change can be selectively monitored by changing the heterodyne phase. In this study, responses of $\Delta n(t)$ were measured throughout the following experiments because transient responses were observed mainly for $\Delta n(t)$, and not for $\Delta k(t)$; theoretical explanations are provided only for $\Delta n(t)$.

In the TG experiments, the refractive index change mainly comes from the release of thermal energy (thermal grating) and from any chemical species that are created or depleted during the course of the photoreaction (species grating) [18]. The signal intensity of the species grating is given by the difference between the change in the refractive index due to the reactant (Δn_r) and that due to the product (Δn_p) when a one-step reaction occurs. Denoting the change in the refractive index due to the thermal grating as Δn_{th}, the NF–HD–TG signal intensity can be written as

$$I(t) = A_1 \Delta n_{\mathrm{th}}(t) + A_2(\Delta n_r(t) - \Delta n_p(t)), \quad (1)$$

where A_1 and A_2 are constants. The sign of Δn_p is negative because the phase of the spatial concentration modulation is shifted by 180° with respect to that of the reactant. The signal intensity of the species grating becomes weaker as the spatial modulations of the

* Corresponding author. Fax: +81 3 3817 1913.
E-mail address: kkata@kc.chuo-u.ac.jp (K. Katayama).

0009-2614/$ - see front matter © 2008 Elsevier B.V. All rights reserved.
doi:10.1016/j.cplett.2008.04.014

refractive index become uniform, and this is accomplished by translational diffusion in a direction perpendicular to the grating. In this case, $\Delta n_r(t)$ and $\Delta n_p(t)$ can be obtained from the diffusion equation for each species, and $I(t)$ is expressed as

$$I(t) = A_1 \Delta n_{\text{th}}^0 \exp(-D_{\text{th}} q^2 t) + A_2 \{\Delta n_r^0 \exp(-D_r q^2 t) - \Delta n_p^0 \times \exp(-D_p q^2 t)\}, \quad (2)$$

where D_{th}, D_r, and D_p are the thermal diffusion coefficient of a solvent and the diffusion coefficients of the reactant and product, respectively, Δn_{th}^0, Δn_r^0, and Δn_p^0 are the initial values of the change in the refractive index due to temperature rise, and concentration changes of the reactant and product, respectively, and q is the grating wave vector equal to $2\pi/\Lambda$, where Λ is the grating spacing.

The photoreduction processes of chlorauric acid proceed step by step according to the following scheme [11]:

$$HAu^{3+}Cl_4 \xrightarrow{h\nu} (HAu^{2+}Cl_3 + Cl) \rightarrow HAu^{3+}Cl_3 + HAu^{+}Cl, \quad (a)$$

$$HAu^{+}Cl \rightarrow (Au^0 + HCl + Cl) \xrightarrow{k_1} \text{seed particle}, \quad (b)$$

$$\text{seed particle} \xrightarrow{k_2} \text{Au nanoparticle}, \quad (c)$$

Different from the above theory explained for the TG signal, not only the reactant ($HAu^{3+}Cl_4$) and product (nanoparticle), but also intermediate species ($HAu^{+}Cl$, seed particle) are involved. $HAu^{2+}Cl_3$ and Au^0 are minor intermediate species. The reduction of HAu^{+} Cl to Au^0atoms and the association of Au^0atoms to form seedparticle concurrently proceeds [19]. There are several reaction channels in the scheme (c) such as coagulation between seed particles and nanoparticles with various sizes, and an average rate constant was used to avoid complicated schemes here. When the reaction occurs in the three steps of the above scheme and the first step finishes faster than the measurement time scale, the equations governing concentration variation are as follows:

$$\begin{aligned}
\frac{\partial[HAu^{3+}Cl_4]}{\partial t} &= D_1 \frac{\partial^2[HAu^{3+}Cl_4]}{\partial x^2}, \\
\frac{\partial[HAu^{+}Cl]}{\partial t} &= D_2 \frac{\partial^2[HAu^{+}Cl]}{\partial x^2} - k_1[HAu^{+}Cl], \\
\frac{\partial[\text{seed}]}{\partial t} &= D_3 \frac{\partial^2[\text{seed}]}{\partial x^2} + k_1[HAu^{+}Cl] - k_2[\text{seed}], \\
\frac{\partial[\text{nanoparticle}]}{\partial t} &= D_4 \frac{\partial^2[\text{nanoparticle}]}{\partial x^2} + k_2[\text{seed}],
\end{aligned} \quad (3)$$

where the square brackets denote the concentration of each species, D_1, D_2, D_3, and D_4 are diffusion coefficients of the trivalent gold species, monovalent gold species, seed particles, and nanoparticles, respectively, and k_1 and k_2 are the rate coefficients of the respective step. These equations were solved under the initial conditions of $[HAu^{+}Cl] = [HAu^{+}Cl]_0$, and $[HAu^{3+}Cl_4] = [HAu^{3+}Cl_4]_0 - [HAu^{+}Cl]_0$. Once the amplitude of the concentration grating (concentration profile of chemical species with a grating pattern) is obtained, $I(t)$ can be expressed as

$$I(t) = A_1 \Delta n_{\text{th}}(t) + A_2 \{\Delta n_1(t) - \Delta n_2(t) - \Delta n_3(t) - \Delta n_4(t)\}, \quad (4)$$

$$\begin{aligned}
\Delta n_1(t) &= \Delta n_1^0 \exp(-D_1 q^2 t), \\
\Delta n_2(t) &= \Delta n_2^0 \exp(-(D_2 q^2 + k_1)t), \\
\Delta n_3(t) &= -\frac{\Delta n_2^0 k_1}{k_1 - k_2 + (D_2 - D_3)q^2} \{\exp(-(D_2 q^2 + k_1)t) - \exp(-(D_3 q^2 + k_2)t)\}, \\
\Delta n_4(t) &= -\frac{\Delta n_2^0 k_1 k_2}{\{k_1 - k_2 + (D_2 - D_3)q^2\}\{k_1 + (D_2 - D_4)q^2\}\{k_2 + (D_3 - D_4)q^2\}} \\
&\quad \times [\{k_1 - k_2 + (D_2 - D_3)q^2\} \exp(-D_4 q^2 t) \\
&\quad - \{k_1 + (D_2 - D_4)q^2\} \exp(-(D_3 q^2 + k_2)t) \\
&\quad + \{k_2 + (D_3 - D_4)q^2\} \exp(-(D_2 q^2 + k_1)t)],
\end{aligned}$$

where Δn_1, Δn_2, Δn_3, and Δn_4 are the modulation amplitudes of the species grating for the trivalent gold species, monovalent gold spe-

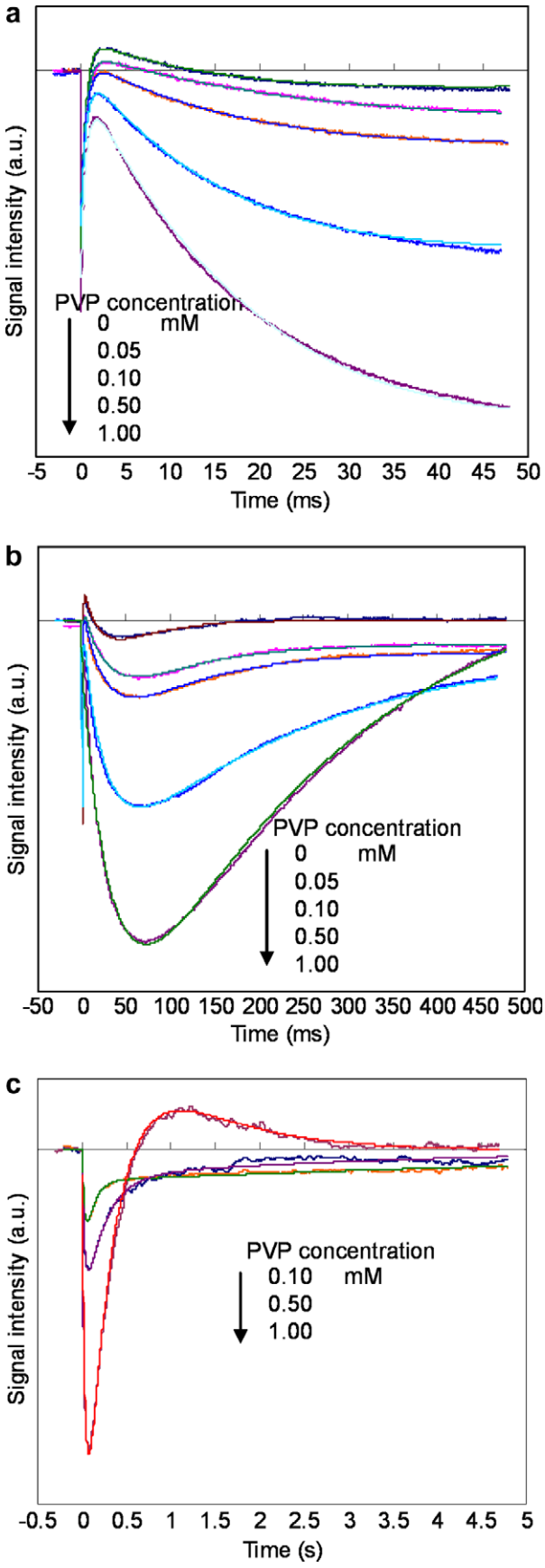

Fig. 1. Dependence of the transient responses obtained by the single-shot NF–HD–TG method as a function of PVP concentration for different time intervals: (a) 0–50 ms, (b) 0–500 ms, and (c) 0–5 s. The grating spacing was 60 μm. Fitting curves were also shown.

cies, seed particles, and nanoparticles, respectively, and Δn_1^0 and Δn_2^0 are the initial modulation amplitudes of the species grating for the trivalent and monovalent gold species, respectively. Provided a decay time for each component of Eq. (4) is τ, a $1/\tau$ vs. q^2 plot gives the diffusion coefficient and rate constant of each species as the slope and intercept of the plot, respectively (q is controllable by the grating spacing) [20]. Eqs. (4) and (5) reveal that the transient response consists of five exponential factors, including a component due to thermal grating, and a sum of exponential decays was used to fit the data, as shown below:

$$I(t) = \sum_i^5 B_i \exp(-t/\tau_i). \quad (6)$$

The optical setup was the same as the one previously reported [19] except that the pump light was operated in single-shot mode. The wavelengths of the pump and probe light were 355 and 532 nm, respectively. After each pump shot, the sample solution was replaced using a flow cell, or else the irradiation position was changed. An aqueous solution of Tetrachlorauric(III) acid (Kishida Chemicals) at a concentration of 10 mM was used as a sample, and the concentration must be higher than 2 mM to get a data with good S/N ratio by a single-shot measurement. Polyvinylpyrrolidone (PVP) (average molecular weight: 40 000) was used as a protective polymer for the nanoparticles. The absorption spectrum of $HAuCl_4$ has an absorption peak around 320 nm, corresponding to the ligand-to-metal charge transfer (LMCT) band [21]. By an absorption of light of 355 nm, photoreduction of chloroauric acid proceeds [11]. After several shots of the pump pulses irradiation, it was confirmed that nanoparticles were generated by the emergence of the plasmon absorption peak around 520 nm.

Transient responses for $HAuCl_4$ aqueous solutions for different PVP concentrations for the grating spacing 60 μm are shown in Fig. 1, and the fitting parameters are listed in Table 1. In all the transient responses, a decay signal with a time constant of 0.60 ms was observed, which is due to a thermal grating decay [19]. The transient response in the absence of PVP consisted of two exponential decays with different signs in the pre-exponential factors, in addition to the thermal grating decay (B2 and B3 components). Another exponential decay (B4 component) was observed in the presence of PVP, and a further exponential decay whose sign is different from that of the B4 component was observed for PVP concentrations above 0.5 mM.

We believe that these four different exponential decays except the thermal decay (B1 component) are due to the four chemical species listed in the above photoreduction reaction scheme. For $HAuCl_4$ solutions at a PVP concentration of less than 0.5 mM, it was confirmed from the absorption spectrum that gold nanoparticles were not formed after several shots of irradiation by the pump pulse. In this case, there is no change in the refractive index due to gold nanoparticles, and it thus plays no role in the transient responses. Then the transient responses are due to the rest of the species, namely the trivalent and monovalent species and seed particles. Considering that the three species have absorption in the wavelength region shorter than the probe wavelength, the real parts of the refractive index change due to them should have the same sign for the probe wavelength from the Kramers–Kronig relation. Considering the signs for the reactant and product are opposite shown in Eq. (4), the B2 component corresponds to the reactant, namely the trivalent species, and the B3 and B4 components correspond to the intermediate products, namely the monovalent species and seed particles, respectively.

It is known that the formation of nanoparticles tends to occur easily with an increase in PVP concentration [22], and this was confirmed by the emergence of a surface plasmon band caused by several shots of pump pulse irradiation at a PVP concentration above 0.5 mM. From the observation of nanoparticle formation and the photoreduction scheme, it was concluded that the slowest dynamics (B5 component) correspond to the generation and subsequent diffusion of nanoparticles. The B5 component is qualitatively different from the B4 component because the signs of their refractive indices differ.

To confirm the origins of the transient responses, the dependence of the normalized transient responses on the pump intensity was investigated. By varying the pump intensity, the concentration of the generated species can be varied. The exponential decays in the transient responses were caused by diffusion and reaction of chemical species. The decay rate due to the diffusion processes depends only on the type of the chemical species involved and not on the concentrations of the species. However, the diffusion of gold nanoparticles should depend on the concentration of photoreduced gold atoms, because their size change induced by it varies their diffusion coefficient. With regard to the reaction rate in the photoreduction scheme, the reactions are first-order or quasi first-order reactions [11], and should not depend on the concentration of species.

The pump intensity dependences of the transient responses in the absence of PVP and for a PVP concentration of 1.0 mM are shown in Figs. 2 and 3, respectively. In Fig. 2, transient waveforms did not depend on the pump intensity. In Fig. 3, the transient

Table 1
Fitting parameters used for the transient responses for various PVP concentrations

	PVP concentration (mM)				
	0.00	0.05	0.10	0.50	1.00
B1	−0.065	−0.050	−0.050	−0.050	−0.062
τ1 (ms)	0.53	0.60	0.60	0.60	0.60
B2	0.031	0.042	0.044	0.073	0.145
τ2 (ms)	20	34	23	18	24
B3	−0.021	−0.030	−0.031	−0.063	−0.190
τ3 (ms)	48	88	95	235	270
B4	–	−0.0059	−0.0089	−0.0080	–
τ4 (ms)	–	8000	7500	3500	–
B5	–	–	–	–	0.041
τ5 (ms)	–	–	–	–	980

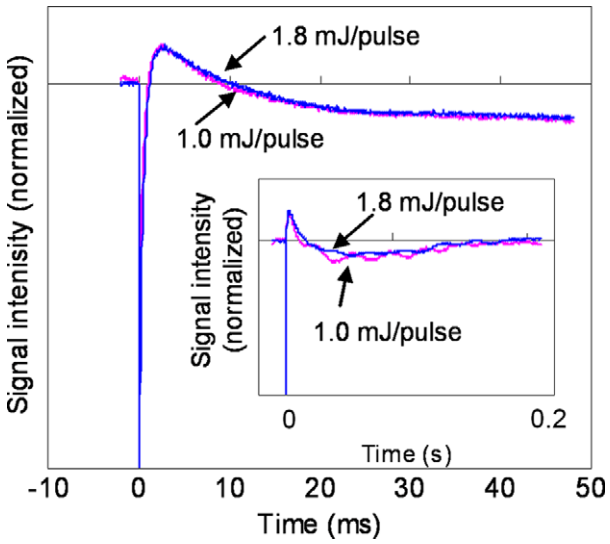

Fig. 2. Pump intensity dependence of the normalized transient responses in the absence of PVP. The pump intensities used were 1.0 and 1.8 mJ/pulse. The transient responses were normalized at the maximum signal intensity. The transient responses for the longer time range are shown in the inset.

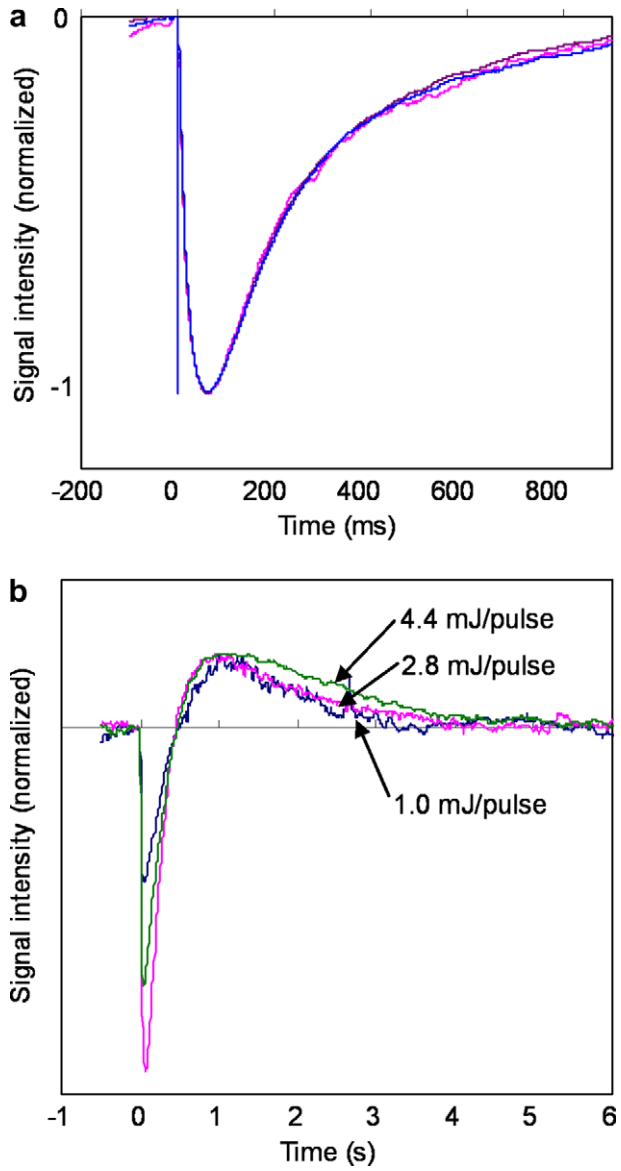

Fig. 3. Pump intensity dependence of the normalized transient responses for a PVP concentration of 1.0 mM for different time intervals: (a) 0–1.0 s and (b) 0–6.0 s. The transient responses were normalized at the intensity of the negative peak around 50 ms for figure (a) and the intensity of the positive signal around 1.0 s for figure (b). In figure (a), all the transient responses almost overlapped with each other.

waveforms within 1.0 s did not depend on the pump intensity, while only the last decay component decayed slower with the pump intensity. The fact that the decay times for the B2, B3, and B4 components did not depend on the pump intensity supports the assumption that the three decay components are originated from the trivalent, monovalent species and seed particles, respectively. The decay time increase in the B5 component strongly supports the conclusion that larger nanoparticles were formed by an increase in the photoreduced gold species and, as a result, diffusion time increased accordingly. In addition, it should be commented that the sign of the B5 component is opposite to the other species components. This indicates that the refractive index change due to nanoparticles is opposite to those for the other species at the probe wavelength of 532 nm. It is probably because the refractive index change was complicatedly changed since the probe wavelength was close to the surface plasmon band.

As was explained in the theory, the diffusion coefficients and rate coefficients in Eq. (5) for each species were obtained from the grating spacing dependence of transient responses, and the results are listed in Table 2. The rate coefficients could not be obtained because the $1/\tau$ vs. q^2 plots intersects at the origin within an error range, and it means that the transient responses were mainly dominated by the diffusion process, not the reaction process. It seems that the rate coefficients for this kind of slow reactions were difficult to obtain by this technique. The diffusion coefficients for the trivalent and monovalent species were smaller as the PVP concentration. Since the diffusion coefficient is inversely proportional to the solvent viscosity and the relative viscosity to water for 0.5 and 1 mM of PVP solutions were 1.53 and 2.23, the dependence of the diffusion coefficient for the trivalent species can be explained by the solvent viscosity change. However, it is supposed that another effect works on the diffusion process of the monovalent gold species because it showed one order decrease by varying the relative viscosity from 1 to 2.23. It is probably due to microscopic interaction between PVP and monovalent gold species [23,24], and not due to the effect of the bulk property although the mechanism is not clear. The diffusion coefficient for seed particles were 1–2 orders smaller than those for trivalent or monovalent gold species, and it is reasonable because the size of the seed particles is much larger than their species. From the diffusion coefficient for nanoparticles, the diameter of the generated nanoparticles was estimated by using the Einstein–Stokes equation and it was 4.8 nm.

Table 2
Diffusion coefficients obtained from the grating spacing dependence of the transient responses for each PVP concentration

	PVP concentration (mM)		
	0.00	0.50	1.00
Dth (m^2/s)	2.0×10^{-7}	2.3×10^{-7}	2.2×10^{-7}
D1 (m^2/s)	7.1×10^{-9}	5.1×10^{-9}	3.8×10^{-9}
D2 (m^2/s)	2.4×10^{-9}	7.4×10^{-10}	2.1×10^{-10}
D3 (m^2/s)	–	1.2×10^{-10}	–
D4 (m^2/s)	–	–	4.9×10^{-11}

The emergence of a signal due to the nanoparticles for PVP concentrations above a threshold value indicates that the nanoparticles were generated only when seed particles is larger than a threshold value by moving step (c) to right. This is supported by the fact that, in general, nanoparticles are only formed when the seed concentration exceeds a threshold value. Another point is that the component for the seed particles were only observed in presence of PVP, and it indicates that PVP stabilizes not only nanoparticles but also seed particles.

Acknowledgement

This research was financially supported by a Grant-in-Aid for Scientific Research from the Japan Society for the Promotion of Science.

References

[1] H. Reiss, J. Chem. Phys. 19 (1951) 482.
[2] V.K. LaMer, R.H. Dinegar, J. Am. Chem. Soc. 17 (1950) 4847.
[3] J.P. Wilcoxon, R.L. Williamson, R. Baughman, J. Chem. Phys. 98 (1993) 9933.
[4] M.Y. Han, C.H. Quek, Langmuir 16 (2000) 362.
[5] S. Inasawa, M. Sugiyama, S. Koda, Jpn. J. Appl. Phys. 42 (2003) 6705.
[6] K. Torigoe, K. Esumi, Langmuir 8 (1992) 59.
[7] K. Kurihara, J. Kizling, P. Stenius, J.H. Fendler, J. Am. Chem. Soc. 105 (1983) 2574.
[8] N. Kometani, H. Doi, K. Asami, Y. Yonezawa, Phys. Chem. Chem. Phys. 4 (2002) 5142.
[9] M. Terazima, J. Photochem. Photobiol. C 3 (2002) 81.
[10] O. Nicolet, E. Vauthey, J. Phys. Chem. A 106 (2002) 5553.
[11] S. Nishida, T. Nada, M. Terazima, Biophys. J. 87 (2004) 2663.
[12] M. Harada, K. Okamoto, M. Terazima, Langmuir 22 (2006) 9142.

[13] K. Katayama, M. Yamaguchi, T. Sawada, Appl. Phys. Lett. 82 (2003) 2775.
[14] M. Yamaguchi, K. Katayama, T. Sawada, Chem. Phys. Lett. 377 (2003) 589.
[15] M. Okuda, K. Katayama, Chem. Phys. Lett. 443 (2007) 158.
[16] M. Okuda, K. Katayama, J. Phys. Chem. A 456 (2008) 47.
[17] T. Tsuruta, M. Okuda, K. Katayama, Chem. Phys. Lett. 456 (2008) 47.
[18] S. Nishida, T. Nada, M. Terazima, Biophys. J. 87 (2004) 2663.
[19] M. Harada, H. Einaga, Langmuir 23 (2007) 6536.
[20] A. Ukai, N. Hirota, M. Terazima, Chem. Phys. Lett. 319 (2000) 427.
[21] A.K. Gangopadhayay, A. Chakravorty, J. Chem. Phys. 35 (1961) 2206.
[22] D.G. Duff, P.P. Edwards, B.F.G. Johnson, J. Phys. Chem. 99 (1995) 15934.
[23] M. Sakamoto, T. Tachikawa, M. Fujitsuka, T. Majima, Langmuir 22 (2006) 6361.
[24] S. Weaver, D. Taylor, W. Gale, G. Mills, Langmuir 12 (1996) 4618.